SCIENTIFIC REPORTS

OPEN

SUBJECT AREAS:
THERMODYNAMICS
SPECTROPHOTOMETRY
KINETICS AND DYNAMICS
METAL COMPLEXES

Received
8 October 2012

Accepted
30 November 2012

Published
21 December 2012

Correspondence and requests for materials should be addressed to Q.K. (kong@synchrotron-soleil.fr)

Microsecond time-resolved energy-dispersive EXAFS measurement and its application to film the thermolysis of $(NH_4)_2[PtCl_6]$

Qingyu Kong[1], Francois Baudelet[1], Jun Han[2], Sebastien Chagnot[1], Laurent Barthe[1], Jon Headspith[3], Roger Goldsbrough[3], Frederic E. Picca[1] & Olivier Spalla[2]

[1]Synchrotron SOLEIL, L'Orme des Merisiers Saint-Aubin, BP 48 91192 Gif sur Yvette Cedex, France, [2]CEA Saclay, DSM/IRAMIS/UMR 3299 CEA/CNRS SIS2M/Laboratoire Interdisciplinaire sur l'Organisation Nanometrique et Supramoleculaire, 91191 Gif sur Yvette, France, [3]Quantum Detectors, Atlas Building, Fermi Avenue, Harwell Oxford, OX11 0QX, UK.

Microsecond (μs) time-resolved extended X-ray absorption fine structure spectroscopy (EXAFS) has been developed using an energy-dispersive EXAFS (EDE) setup equipped with a silicon Quantum Detector ULTRA. The feasibility was investigated with a prototypical thermally driven redox reaction, the thermal decomposition of $(NH_4)_2[PtCl_6]$. EXAFS data were collected with snapshots every 60 μs during the course of the thermolysis reaction, then averaged for 100 times along the reaction to get better signal to noise ratio which reduces the time resolution to 6 millisecond (ms). Our results provide direct structural evidence of cis-$PtCl_2(NH_3)_2$ as the intermediate, together with continuous electronic and geometric structure dynamics of the reactant, intermediate and final product during the course of the thermolysis of $(NH_4)_2[PtCl_6]$. The thermal effect on EXAFS signals at high temperatures is considered in the data analysis, which is essential to follow the reaction process correctly. This method could also be applied to other reaction dynamics.

The time to measure an EXAFS spectrum has been improved dramatically from minutes in the early days to seconds with quick EXAFS (QEXAFS)[1,2] and milliseconds with EDE[3,4]. Microsecond EDE has only recently become accessible with the advent of the fast readout silicon Quantum Detectors ULTRA and the high brilliance third generation synchrotron radiation sources[5,6]. The time domain for chemically or thermally driven reactions could vary from hours to ultrafast regime when atomic or electronic motions are the dominant effect. Representatives are catalytic process[7], formation of metal nanoparticles[8,9] and thermolysis dynamics[10,11] and such reactions are well suited for time-resolved EDE studies.

We have applied microsecond EDE (μs-EDE) to the thermolysis of di-ammonium hexachloroplatinate, $(NH_4)_2[PtCl_6]$, which was predicted to first undergo an internal redox reaction forming an intermediate, which subsequently completely decomposes to metallic Pt. $(NH_4)_2[PtCl_6]$ has been shown to be a good precursor to obtain metallic Pt through thermolysis due to its low decomposition temperature[12]. The thermolysis mechanism has been investigated extensively[13–16] including time-resolved EDE at the Cl K-edge and Pt L_3 edge with a time resolution of 10 seconds[10], and several intermediates such as $PtCl_4$[14], $PtCl_6$[15] and cis-$PtCl_2(NH_3)_2$[10], have been proposed. However, despite these numerous studies[10,13–16], direct structural evidence for the intermediate and the reaction dynamics have been lacking. Here, microsecond time-resolved EDE provided direct structural evidence of cis-$PtCl_2(NH_3)_2$ as the intermediate, together with detailed reaction dynamics.

Results

Data analysis. The single shot EXAFS spectrum of $(NH_4)_2[PtCl_6]$ at the onset of the measurement with a time resolution of 60 μs is shown in Figure 1a, which is good enough to follow the signal changes by analyzing the XANES region but maybe too noisy to obtain consistent structural parameters from detailed EXAFS analysis. To increase the signal to noise ratio, the thermal decomposition reaction of $(NH_4)_2[PtCl_6]$ was repeated for 15 times with the same experimental conditions. The experimental data at the same time delays of each separate reaction were averaged without changing the time resolution. The averaged spectrum from 15 reactions at the onset of the measurement with a time resolution of 60 μs is shown in Figure 1b, all the averaged spectra during the course of

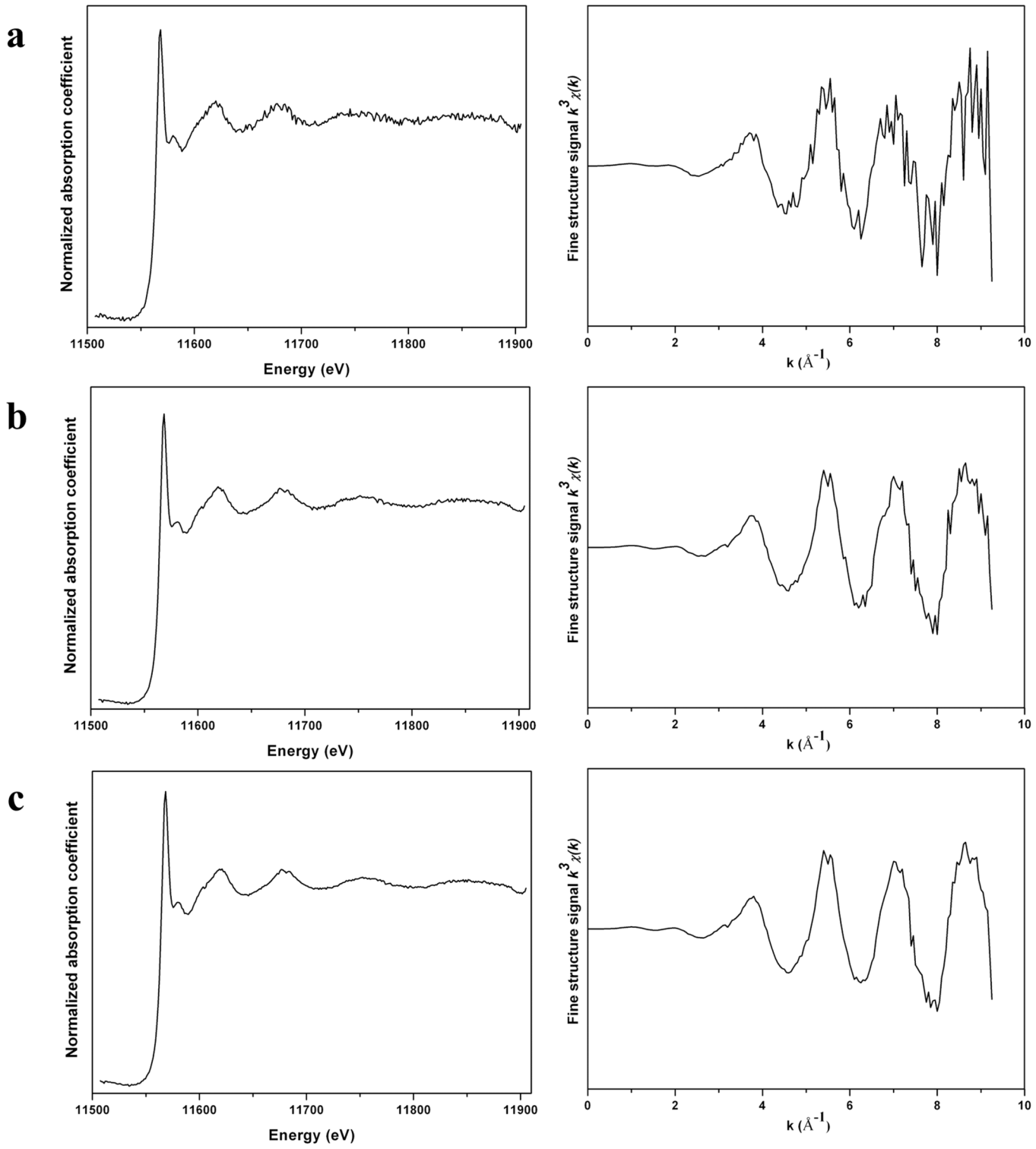

Figure 1 | Single shot and averaged experimental EXAFS spectra. a. The single shot EXAFS spectrum at the onset of the measurement with a time resolution of 60 μs. b. Averaged EXAFS spectrum from 15 separate measurements with a time resolution of 60 μs. c. 1500 times averaged EXAFS spectrum with a time resolution of 6 ms. The normalized absorption coefficient χ_μ(E) (left) and the fine structure signal $k^3\chi(k)$ (right).

the reaction are shown in a two dimensional image in Figure S1 in the supplementary information (SI). An initial data analysis, aimed to search new intermediates with short lifetime at the onset of the reaction, was carried out from 300 to 330°C using 3×10^6 spectra with a time resolution of 60 μs which were averaged from 15 reactions. After confirmed that only cis-$PtCl_2(NH_3)_2$ is formed as intermediate and realized that 60 μs is much faster than the speed of the thermolysis reaction from the first analysis, 3×10^7 EXAFS spectra collected from 208 to 508 ± 5°C were averaged every 100 spectra along the reaction to further increase the signal-to-noise level. Finally, 3×10^5 spectra averaged for 1500 times with a time resolution of 6 ms were used for the second data analysis, which are shown in Figure 2a to illustrate the continuous evolution of the EXAFS signals during the course of the reaction. The normalized absorption coefficient $\chi_\mu(E)$ and the fine structure signal $k^3\chi(k)$ at the onset of the measurement is shown in Figure 1c to demonstrate the

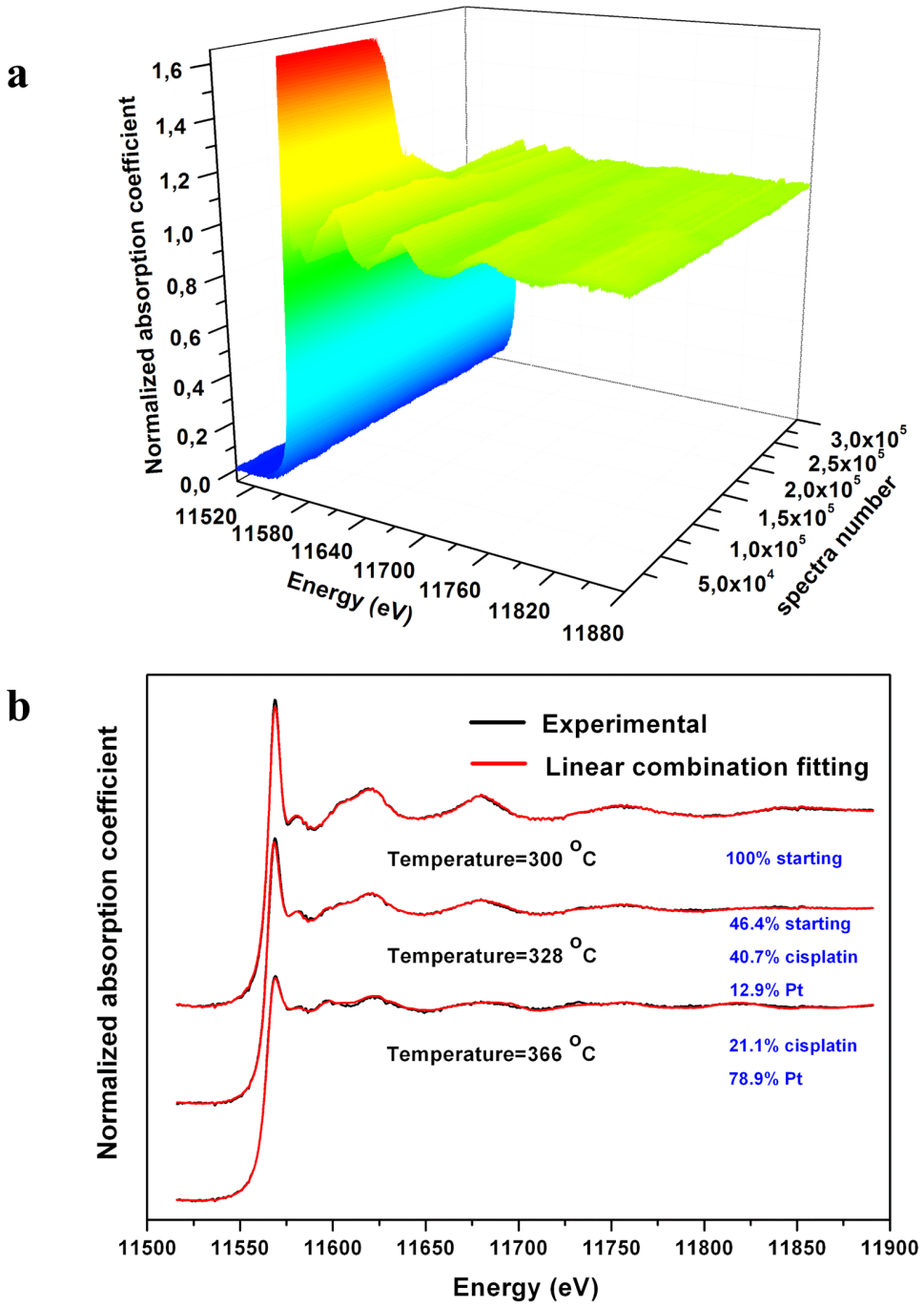

Figure 2 | Experimental EXAFS spectra used to follow the reaction dynamics of the thermolysis of $(NH_4)_2[PtCl_6]$. a. The averaged 3×10^5 EXAFS spectra with a time resolution of 6 ms, illustrating continuous evolution of EXAFS signal during the course of the reaction. b. Selected experimental EXAFS spectra (black curves) at the onset, in the middle and at the late stage of the reaction, together with linear combination fitting with reference spectra (red curves).

quality of the data, and selected absorption spectra at various reaction stages are shown in Figure 2b to illustrate the signal changes. What need to be noted is that there are several Bragg peaks in the transmitted intensity after the sample and in I0 at the Pt L_3 edge (11563.7 eV), which come from the Si311 monochromator. Since our I0 is only measured once before the reaction, one of the Bragg peaks in the transmitted intensity is not compensated completely by that in I0 due to slight perturbation of the X-ray beam during the course of the measurement, producing a glitch in the middle of the EXAFS spectra. A Python deglitch program, which is similar to the deglitch function in Athena, is used to remove the glitches by setting appropriate tolerance values and energy ranges.

The experimental data were analyzed using linear combination fitting (LCF) with reference spectra, to obtain the structural dynamics of the reactant, intermediates and product in the course of the reaction. The initial molecule $(NH_4)_2[PtCl_6]$ could decompose through three possible channels: (i) cis-$PtCl_2(NH_3)_2$ or trans-$PtCl_2(NH_3)_2$ plus 2HCl and 2Cl, (ii) $PtCl_6 + 2NH_3 + H_2$, and (iii) $PtCl_4 + NH_3 + HCl + NH_4Cl$. Because the EXAFS data is element specific, only those molecules containing Pt atoms could be detected at the Pt L_3 edge and were considered as possible intermediates in the data analysis, while molecules such as HCl, NH_3, and NH_4Cl are not included in the analysis. In summary the EXAFS spectra of following molecules are measured and used as references in the analysis:

$(NH_4)_2[PtCl_6]$, cis-$PtCl_2(NH_3)_2$, trans-$PtCl_2(NH_3)_2$, $PtCl_4$, and metallic Pt. Since $PtCl_6$ does not exist and the only similar compound PtF_6, in which the oxidation state of platinum is Pt^{6+}, is volatile and cannot be measured at high temperature, the reference spectrum of $PtCl_6$ is lacking. The formation of $PtCl_6$ in the course of the thermolysis reaction is excluded from the electronic structure dynamics which is shown below in Figure 5. Due to the increase in anharmonic vibrations and disorder in the lattice structure of the compound, which results in asymmetry of the pair distribution functions, the EXAFS signals are dampened at high temperature[17–19]. Since the experiment was carried out between 208 to 508°C, the reference spectra of the above mentioned molecules were also measured at high temperatures to take into account the thermal effect. Our results illustrate that the starting material $(NH_4)_2[PtCl_6]$, cis-$PtCl_2(NH_3)_2$, trans-$PtCl_2(NH_3)_2$, and $PtCl_4$ decompose after 315°C, 268°C, 265°C and 366°C, respectively, based on which the absorption spectra at 300°C for the starting material, 250°C for cis-$PtCl_2(NH_3)_2$ and trans-$PtCl_2(NH_3)_2$, and 350°C for $PtCl_4$ are used as references in the data analysis. Figure 3a shows the comparison of the absorption spectra of the above mentioned molecules at chosen and ambient temperatures. The signals of the starting molecule at 300°C and $PtCl_4$ at 350°C dampen conspicuously, while there is only slightly change for

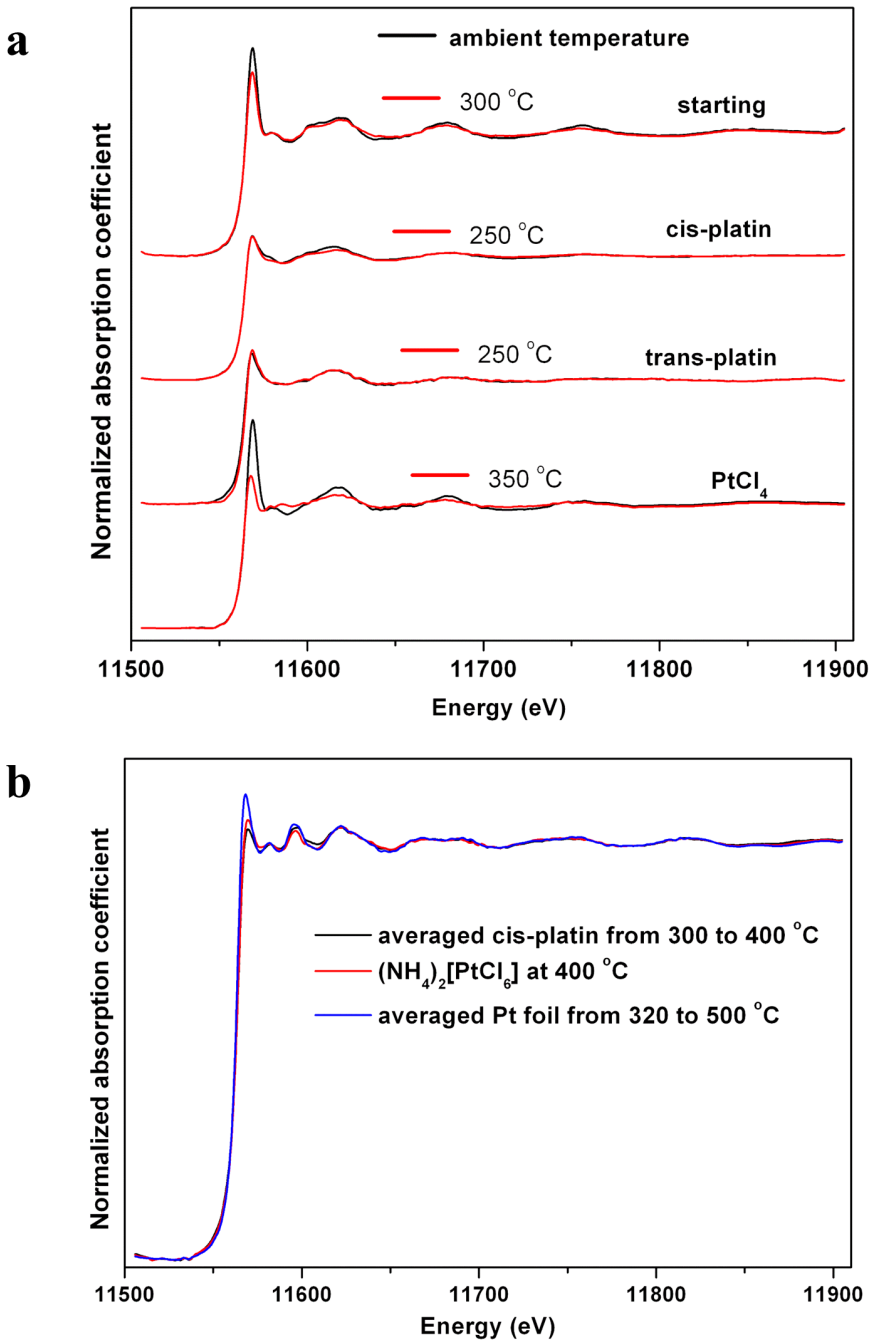

Figure 3 | Reference experimental EXAFS spectra used in LCF analysis. a. Comparison of the measured reference absorption spectra at ambient (black) and high temperatures (red): the starting molecule $(NH_4)_2[PtCl_6]$ at 300°C, cis-$PtCl_2(NH_3)_2$ at 250°C, trans-$PtCl_2(NH_3)_2$ at 250°C and $PtCl_4$ at 350°C, from top to bottom. b. the reference absorption spectra for metallic Pt: averaged Pt foil measured from 320 to 500°C (blue), the starting molecule $(NH_4)_2[PtCl_6]$ measured at 400°C after the thermal decomposition completed and only metallic Pt exist (red), and averaged absorption spectra of cis-$PtCl_2(NH_3)_2$ measured from 300 to 400°C (black).

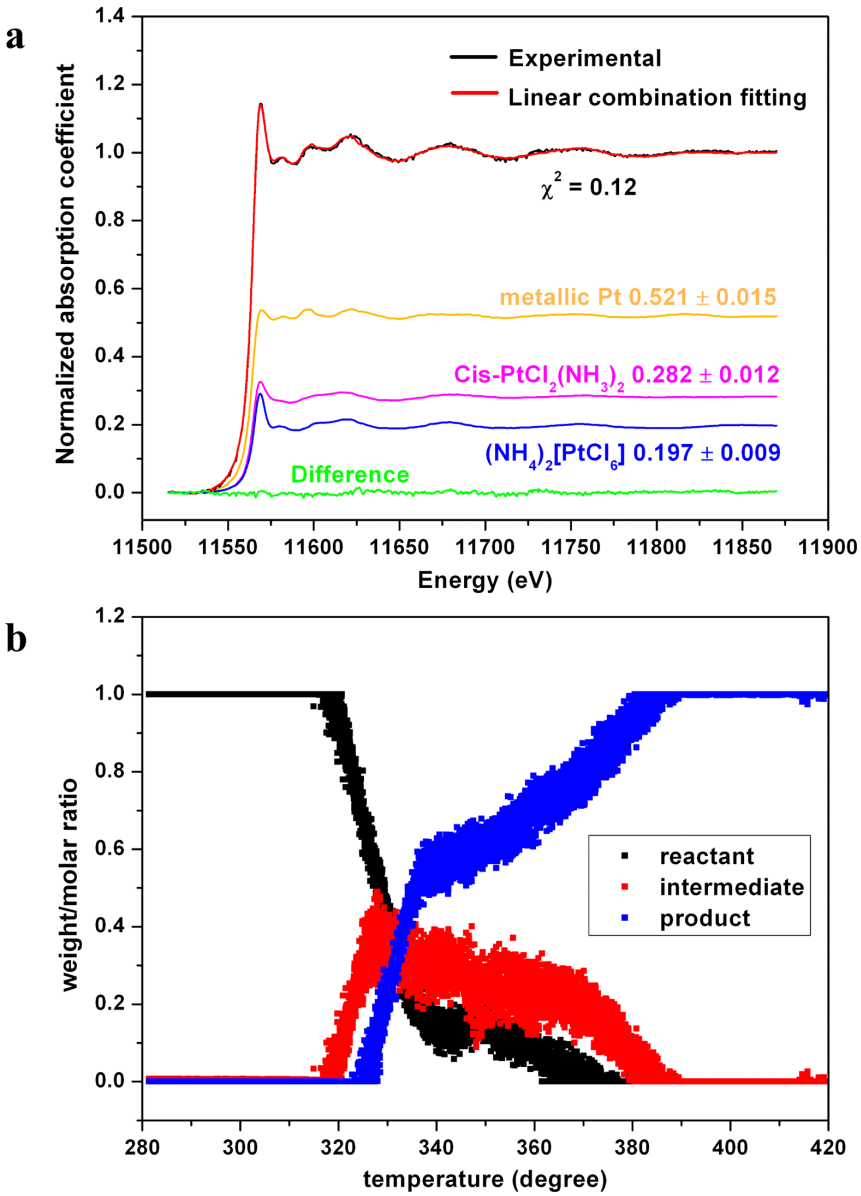

Figure 4 | Structural dynamics of the reactant, intermediate and product in the course of the thermal decomposition of $(NH_4)_2[PtCl_6]$. The experimental data are fitted linearly with experimental reference EXAFS spectra shown in Figure 3, using a least square refinement algorithm. The molar ratios of the references are optimized freely in the LCF until a best fit with minimum figure of merit value (χ^2) is obtained. Our results illustrate that only the starting molecule at 300°C, cis-$PtCl_2(NH_3)_2$ at 250°C and the averaged absorption spectra of cis-$PtCl_2(NH_3)_2$ measured from 300 to 400°C survive in the LCF, while the concentration of the other species converges to zero. a. The experimental (black) and fitted (red) EXAFS spectra at 335°C are shown to demonstrate the linear combination fitting process. Also shown are components and their corresponding molar ratio: reactant $(NH_4)_2[PtCl_6]$ at 300°C (blue), intermediate cis-$PtCl_2(NH_3)_2$ at 250°C (magenta), and product metallic Pt (orange). b. The evolution of the populations of the reactant $(NH_4)_2[PtCl_6]$, intermediate cis-$PtCl_2(NH_3)_2$, and the final product metallic Pt, as a function of the reaction temperature.

cis-$PtCl_2(NH_3)_2$ at 250°C and the signal of trans-$PtCl_2(NH_3)_2$ at 250°C is almost identical to that at ambient temperature.

The absorption spectra of Pt foil change significantly from ambient temperature to 320°C, while are almost identical between 320 and 500°C as shown in Figure S2 in SI. Since the phase transition of Pt is around 2000°C[20], the EXAFS signal changes of Pt foil before 500°C come only from the thermal disorder, the spectra of Pt foil measured between 320 and 500°C are averaged and used as reference in the data analysis. It is most probably, however, that small nanoparticles of Pt are formed at the onset of the thermolysis reaction which then nuclear progressively to bulk entities during the course of the reaction[21,22], the EXAFS signal of metal nanoparticles are different from that of bulk foil since the nanoparticles generally have dispersed or disordered structures with asymmetry pair distribution functions[18,23] and the atom-atom distance could also be quite different from that in well-defined bulk structure[17]. The absorption spectrum of Pt foil alone cannot reproduce the signals of metallic Pt formed in the thermolysis reaction, which could be in the form of small clusters or a mixture of nanoparticles and bulk entities. The absorption spectrum of the starting molecule $(NH_4)_2[PtCl_6]$ at 400°C, after the thermal decomposition reaction completed and only metallic Pt exist, is used as the second reference spectrum for metallic Pt. Since the thermal decomposition reaction starts at 315°C and finishes before 400°C, the absorption spectrum of the fully reduced sample at 400°C may not represent precisely the signals of metallic Pt during the course of the reaction, another measurement on cis-$PtCl_2(NH_3)_2$ was carried out at high temperatures after the decomposition point. From our measurement cis-$PtCl_2(NH_3)_2$ starts to

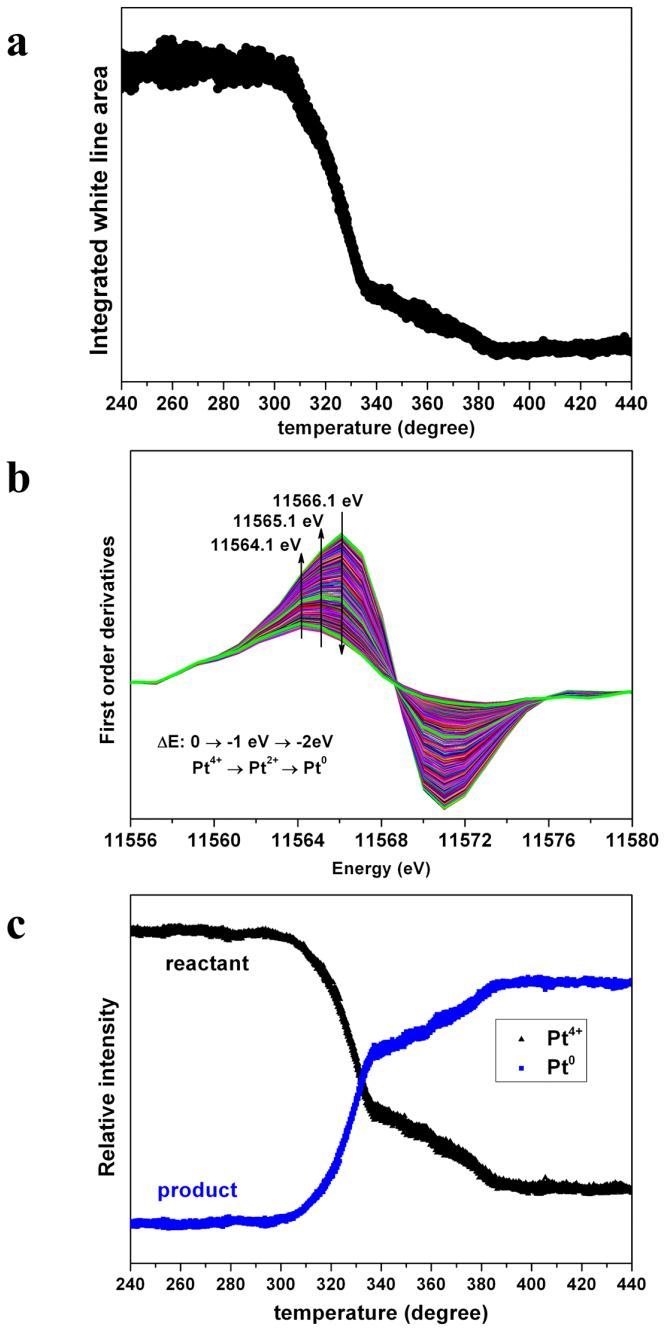

Figure 5 | Valence electronic structure dynamics during the course of the thermal decomposition of $(NH_4)_2[PtCl_6]$. a. The integrated white line area decreases exponentially demonstrating the continuous decrease of the unoccupied density of states of the absorbing atom Pt in the course of the reaction. b. The first order derivatives displays three homogenously separated peaks at 11566.1, 11565.1 and 11564.1 eV, respectively, with a total energy shift of 2 eV at the end of the reaction. The peak at 11566.1 eV dominates at the onset of the reaction and decreases gradually and disappears at the end of the reaction, it is assigned to the rising edge of Pt^{4+} of the reactant $(NH_4)_2[PtCl_6]$. The second peak at 11565.1 eV appears in the middle of the reaction and is assigned to the rising edge of Pt^{2+} of the intermediate cis-$PtCl_2(NH_3)_2$. The peak at 11564.1 eV dominates at the end of the reaction and is assigned to the rising edge of Pt^0 of metallic Pt. c. evolution of the relative peak intensities at 11566.1 eV and 11564.1 eV in (b), as a function of temperature, illustrating the decomposition of the reactant and formation of the final product in the course of the reaction. Due to the overlap, the relative peak intensity at 11565.1 eV for the intermediate is almost constant, and not included in the figure. The integrated white line intensity and the relative intensities of the first order derivatives display discontinuities at 335°C instead of a single-step evolution, revealing the existence of intermediates during the course of the reaction. The white line intensities and the first order derivatives are direct experimental data and fingerprints to illustrate the electronic structural dynamics during the course of the thermolysis reaction. The formation of $PtCl_6$, in which the oxidation state of the platinum (Pt^{6+}) is higher than that in the starting molecule (Pt^{4+}), is ruled out from our results which illustrate a continuous decrease of the oxidation state of the platinum atom in the reaction.

decompose at 268°C and the EXAFS spectra between 300 and 400°C are almost identical and represent the characteristic of metallic Pt as shown in Figure S3, which are averaged and used as the third reference for metallic Pt. In summary three absorption spectra that come from bulk material and small clusters of Pt are used as references for metallic Pt in the data analysis: the Pt foil measured at high temperature between 300 and 500°C, the EXAFS spectra of $(NH_4)_2[PtCl_6]$ at 400°C and cis-$PtCl_2(NH_3)_2$ between 300 and 400°C, which are shown in Figure 3b.

Geometric structure dynamics. Figure 4a illustrates the LCF process with a least-square refinement algorithm[24]. The fit yields the weight (or mole ratio) of the reactant, putative intermediates and product. By fitting the experimental EXAFS data at each reaction step as illustrated in Figure 2b, the population evolution of different molecules involved in the reaction could be followed in real time. Figure 4b shows the structural dynamics of the reactant, intermediate and the final product, as a function of the reaction temperature. Different reaction dynamics was obtained when the absorption spectra of $(NH_4)_2[PtCl_6]$, cis-$PtCl_2(NH_3)_2$, trans-$PtCl_2(NH_3)_2$, $PtCl_4$ and Pt foil measured at ambient temperature were used as references, the result is shown in Figure S4.

Electronic structure dynamics. A big advantage of EXAFS is that the valence electronic and the geometric structure about the absorbing atoms can be obtained simultaneously in a single spectrum[25]. The white line intensity that reflects the unoccupied density of states and the rising edge that reflects the excitation of core electrons to the ionization threshold could be used as fingerprints to show the valence electronic structural dynamics in the course of a chemical reaction. Figures 5a and 5b illustrate the changes of the integrated white line area and the first order derivatives, respectively, during the course of the thermolysis reaction of $(NH_4)_2[PtCl_6]$. For the first order derivatives, three homogeneously separated peaks are observed and evolve with the reaction process, the changes of the relative intensities of the first and last appeared peaks during the course of the reaction are shown in Figure 5c.

Elucidation of the intermediate. During the LCF, all the reference spectra measured at high temperatures as shown in Figure 3 were included and the concentration of each specie was evaluated freely using the least-square refinement algorithm until a best fit with minimum figure of merit value (χ^2) was obtained[24,26,27]. Our results illustrate that only the starting molecule at 300°C, cis-$PtCl_2(NH_3)_2$ at 250°C and the averaged absorption spectra of cis-$PtCl_2(NH_3)_2$ measured from 300 to 400°C survive in the LCF, while the concentration of the other species converges to zero. The fitting result of a selected EXAFS spectrum at 335°C was shown as an example in Figure 4a to illustrate the fitting process. To determine the molecular structure of the intermediate and compare with Figure 4a, similar fittings using trans-$PtCl_2(NH_3)_2$ or $PtCl_4$ only as the intermediate were made and shown in Figure 6a and b.

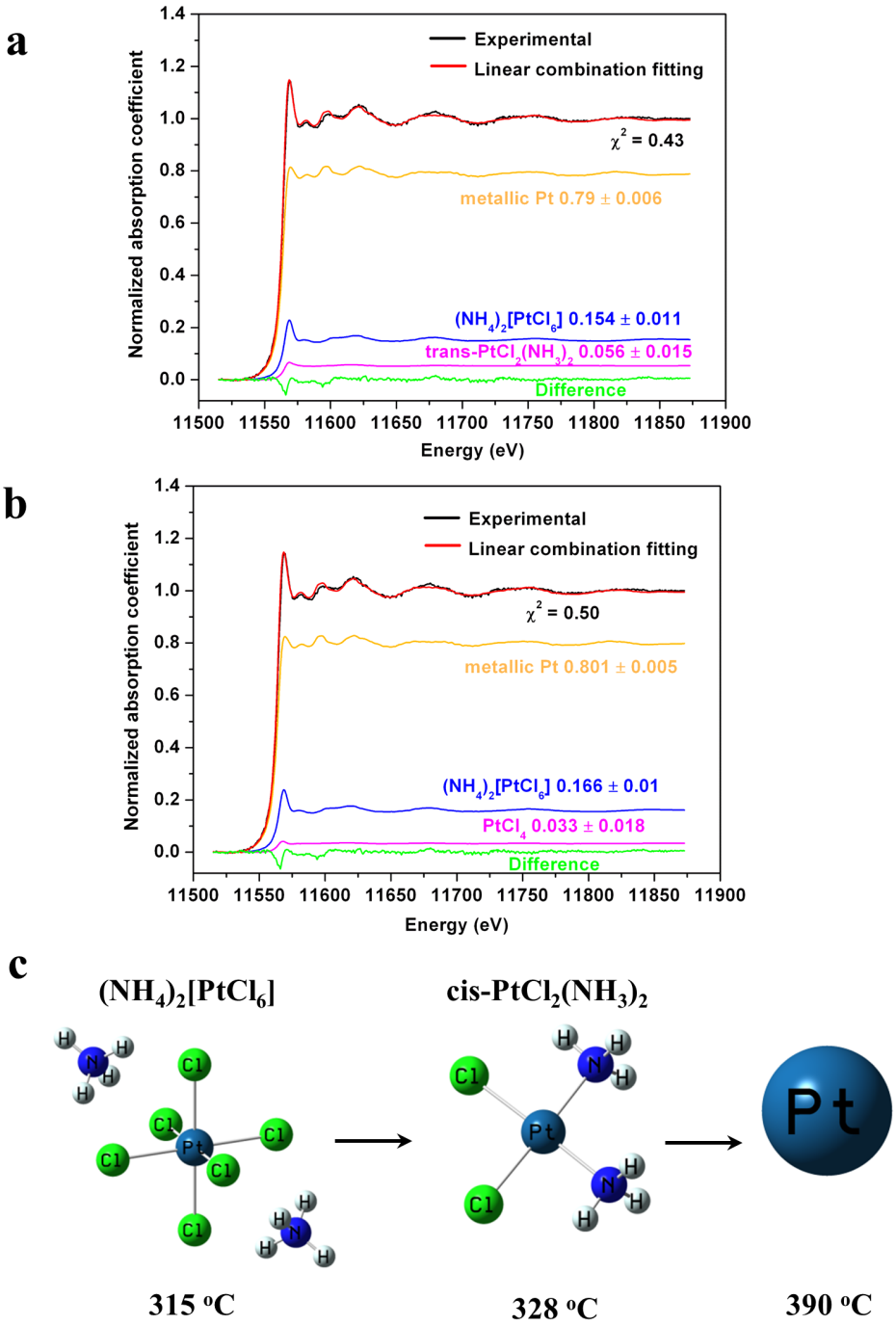

Figure 6 | Determination of cis-$PtCl_2(NH_3)_2$ as intermediate. To compare with Figure 4a, in which all the reference spectra as shown in Figure 3 are included in the LCF and only cis-$PtCl_2(NH_3)_2$ remains as the intermediate after the least square refinement calculation, similar fittings using trans-$PtCl_2(NH_3)_2$ or $PtCl_4$ only as the intermediate were made: the experimental (black) and fitted (red) EXAFS spectra at 335°C using a. trans-$PtCl_2(NH_3)_2$ or b. $PtCl_4$ only as the intermediate. Also shown are components and their corresponding molar ratio: reactant $(NH_4)_2[PtCl_6]$ at 300°C (blue), intermediate trans-$PtCl_2(NH_3)_2$ at 250°C (magenta) or $PtCl_4$ at 350°C (magenta), and product metallic Pt (orange), as well as the difference between the experimental and fitted spectra (green). The figure of merits χ^2 in Figure 4a, Figure 6a and Figure 6b illustrate that cis-$PtCl_2(NH_3)_2$ fit the experimental data better and is the most likely intermediate formed during the thermolysis reaction of $(NH_4)_2[PtCl_6]$. The difference curves in green also give a visual impression that cis-$PtCl_2(NH_3)_2$ fit the experimental data better than trans-$PtCl_2(NH_3)_2$ or $PtCl_4$. The concentrations of trans-$PtCl_2(NH_3)_2$ (5.6%) and $PtCl_4$ (3.3%) as shown in Figure 6a and b are close to the error bar of the single-to-noise ratio of our data, illustrating that trans-$PtCl_2(NH_3)_2$ and $PtCl_4$ are minor reaction channels compared to cis-$PtCl_2(NH_3)_2$ and can be neglected. c. Schematic reaction mechanism based on microsecond (μs) time-resolved EDE results.

Discussion

Our results in Figure 4b illustrate that the decomposition of the parent molecule $(NH_4)_2[PtCl_6]$ starts at 315°C and finishes at 370°C with a time constant of 5.5 minutes, the population of the starting molecule decays exponentially with two steps separated at 335°C with reaction rate constants of 0.015/s and 0.005/s respectively, which illustrates the existence of intermediates during the course of the reaction. The intermediate cis-$PtCl_2(NH_3)_2$ is formed simultaneously at the onset of the reaction, its population reaches a maximum at 328°C with a rate constant of 0.046/s then decays completely to the final products at 390°C in two steps separated at 370°C with rate constants of 0.004/s and 0.025/s,

respectively. Metallic Pt is formed 1 minute after the intermediate at 325°C and its population increases with a two-step exponential function with reaction rate constants of 0.042/s and 0.002/s, after 390°C metallic Pt is the only Pt-species in the sample. The calculation of the rate constant and the results are shown in Table s1 in SI. Our analysis reveals that of three references for metallic Pt as shown in Figure 3b, only the averaged absorption spectrum of cis-$PtCl_2(NH_3)_2$ between 300 and 400°C survives in the LCF, while the others converge to zero. Although it is not the topic of the present study, the metallic Pt formed during the course of the thermolysis of $(NH_4)_2[PtCl_6]$ is most probably in the form of nanoparticles since the formation of bulk Pt is ruled out from our analysis.

Different structural dynamics was obtained with reference spectra measured at ambient temperature and Pt foil only without considering the formation of Pt nanoparticles, as shown in Figure S4 in SI. The major differences are: the population of the starting molecule decays with a single-step exponential function with a shorter lifetime of 2 minutes and, the intermediate appears 1 minute after the metallic Pt which is formed at the onset of the reaction. Formation of an intermediate after the final product is not reasonable, and the single-step exponential decay of the starting molecule, which illustrates that the formation of an intermediate is not likely, is contradict to the formation of cis-$PtCl_2(NH_3)_2$ and the two-step thermolysis reaction process. Our results strikingly illustrate that considering the thermal effect in the data analysis is essential to follow the reaction process correctly. Although the structural dynamics in Figure 4b might be slightly different from its real reaction, since the reference spectra of the starting molecule at 300°C, the cis-$PtCl_2(NH_3)_2$ and trans-$PtCl_2(NH_3)_2$ at 250°C are not exactly in the temperature range of the reaction between 315 and 390°C, it is the most precise result we could obtain at present report. Previous EDE study at the Cl K-edge and Pt L_3 edge also provided information about the starting point of the reaction and proposed the structure of the intermediate. However, due to the limited time resolution of 10 seconds and only XANES signals were measured and compared with the reference spectrum measured at ambient temperature, no conclusive results could be obtained[10].

Figure 5a illustrates that the integrated white line intensity decays exponentially in two steps separated at 335°C, illustrating the continuous decrease of the unoccupied density of states of the absorbing atom Pt, as well as the existence of intermediates during the course of the thermolysis reaction. The first order derivatives of the EXAFS spectra, which are direct measurements of the rising edges, displays three peaks at 11566.1, 11565.1 and 11564.1 eV, respectively, with an homogenous energy shift (ΔE) of −1.0 eV as shown in Figure 5b. The peak at 11566.1 eV which dominates at the onset of the reaction and then decays gradually and completely disappears at the end of the reaction, is assigned to the rising edge of Pt^{4+} of the initial molecule $(NH_4)_2[PtCl_6]$. The peak at 11565.1 eV only appears in the middle of the reaction and disappears at the end, it is assigned to the rising edge of Pt^{2+} in cis-$PtCl_2(NH_3)_2$. At the end of the reaction, the peak at 11564.1 eV dominates and is assigned to the rising edge of metallic Pt^0. Figure 5c shows the changes of relative intensities of the first order derivative signals at 11566.1 and 11564.1 eV. Consistent with the geometric dynamics (Figure 4b), the valence electronic dynamics also reveals the gradual decomposition of the starting material and formation of the final product. The discontinuity in the change of the relative intensities at 335°C as shown in Figure 5c, illustrates again the existence of intermediates during the course of the reaction, which confirms our assignment of the peak at 11565.1 eV to the rising edge of Pt^{2+} in cis-$PtCl_2(NH_3)_2$. Previous thermal gravimetric analysis (TGA) showed that the thermal decomposition take place in two steps and suggested $PtCl_6$ as the intermediate[15,28], however our results (Figure 5) clearly illustrate the continuous decrease of the oxidation states of Pt during the course of the reaction, the formation of $PtCl_6$ in which the oxidation state of platinum is Pt^{6+} could be a minor reaction channel and is negligible. Our results of geometric and electronic structural dynamics clearly illustrate the two-step reaction process during the thermal decomposition reaction: $(NH_4)_2[PtCl_6]$ $(Pt^{4+}) \rightarrow$ cis-$PtCl_2(NH_3)_2$ $(Pt^{2+}) \rightarrow$ metallic Pt^0.

The comparison of the fitting qualities among Figure 4a, Figure 6a and Figure 6b illustrates that cis-$PtCl_2(NH_3)_2$ is the most likely intermediate formed in the thermolysis of $(NH_4)_2[PtCl_6]$. The residues between the experiment and fitting (green curves in Figures 4a, 6a and 6b) as well as the figure of merit (χ^2) confirm that cis-$PtCl_2(NH_3)_2$ fits the data better than the other compounds. More importantly, if a mixture of all intermediates, cis-$PtCl_2(NH_3)_2$, trans-$PtCl_2(NH_3)_2$, and $PtCl_4$ are included simultaneously in the fit, only cis-$PtCl_2(NH_3)_2$ remains after least-square refinement, the fraction of other components converges to zero. Furthermore, the concentrations of trans-$PtCl_2(NH_3)_2$ (5.6%) and $PtCl_4$ (3.3%) are quite low, which are close to the error bar of the single-to-noise ratio of our data as shown in Figures 6a and b, illustrating that trans-$PtCl_2(NH_3)_2$ and $PtCl_4$ could not be detected from our current measurement and their formations are minor reaction channels compared to cis-$PtCl_2(NH_3)_2$ and is negligible.

The detection of cis-$PtCl_2(NH_3)_2$ as the intermediate molecule, together with detailed electronic and geometric structure dynamics of involved molecules during the course of the thermal decomposition reaction of $(NH_4)_2[PtCl_6]$, which has escaped from previous studies, strikingly illustrates the capability of μs-EDE to film continuously a chemical reaction process in real time.

Methods

The experiment was carried out at the ODE beamline at Soleil Synchrotron[5] at the Pt L_3 edge using the Si311 monochromator with an intrinsic Darwin width of 0.5 eV at Pt L_3 edge, which produces a flux of 1×10^9 photons s^{-1} eV^{-1}. It is important to use Si311 with better energy resolution to get clear white line signals which are used as fingerprints to obtain the electronic structural dynamics during the course of the thermolysis reaction. The comparison of the XANES spectra measured with Si311 and Si111 are shown in Figure S5 in SI. A focus spot of 60 × 35 μm (horizontal × vertical) was obtained with the focusing mirror and the monochromator. The silicon ULTRA detector (Quantum Detectors, Harwell Oxford, UK) with 512 × 1 (horizontal × vertical) pixels and a pixel size of 50 μm[5,6] was used to measure the EXAFS spectra in transmission mode. The energy resolution of our measured absorption spectrum, which is controlled by several parameters[29,30], is obtained to be 0.89 eV through a convolution calculation of a reference spectrum with known energy resolution, and the detailed calculations are described in the caption of Figure S6 in SI. The detector was operated in the external trigger mode at a repetition rate of 20 KHz, corresponding to a readout time of 50 μs, which overlaps with the integration time during the data collection to increase the time resolution. There is an additional reset time of 1.1 μs between successive spectra, an integration time of 58.9 μs is used for the measurement to obtain a time resolution of 60 μs (the time resolution equals the integration time plus reset time plus the readout time, which overlaps with the integration time of 58.9 μs and can be neglected). The upgraded control program allows to record a sequence of 7×10^7 frames continuously, producing a predefined data matrix of 72 GB. Detailed descriptions of the silicon quantum detector are given in previous reports[5,6]. A complete EXAFS spectrum with an overall energy range of 390 eV at the Pt L_3 edge could be obtained with a single exposure to the detector. The starting di-ammonium hexachloroplatinate (99.999%) and reference samples cis-$PtCl_2(NH_3)_2$ (99.9%), trans-$PtCl_2(NH_3)_2$, and $PtCl_4$ (99.99%) were purchased from Sigma Aldrich and used directly without further purifications. A water cooled oven[31] was used to heat the sample up to 600°C at a rate of 10°C/minute, helium gas was flowed through the sample to avoid oxidations. The powders of the starting molecule, cis-$PtCl_2(NH_3)_2$, trans-$PtCl_2(NH_3)_2$ and $PtCl_4$ were diluted using graphite powder with volume ratios of 1 : 8, 1 : 7, 1 : 7 and 1 : 9, respectively, to have an optimal absorption jump around 1 at the Pt L_3 edge. The mixed sample was pressed homogeneously into the sample holder of the oven with a thickness of 2 mm, which is sealed using graphite foil with a thickness of 125 μm on both sides. Metallic Pt at ambient temperature was measured before and after the reaction for energy calibration.

A Windows C++ program from Quantum Detectors was used to extract text files from the data matrix and make the average. The normalization, LCF, white line integration, first order derivative calculations and deglitch of the EXAFS spectra were carried out with homemade Python programs.

1. Frahm, R. New method for time-dependent X-ray absorption studies. *Rev. Sci. Instrum.* **60**, 2515–2518 (1989).

2. Dobson, B. R. Quick scanning Exafs facilities at Daresbury SRS. *Syn. Rad. News* **7**, 21–24 (1994).
3. Phizackerley, R. P. *et al*. An energy-dispersive spectrometer for the rapid measurement of X-ray absorption spectra using synchrotron radiation. *J. Appl. Cryst.* **16**, 220–232 (1983).
4. Dartyge, E. *et al*. X-ray absorption in dispersive mode – A new spectrometer and a data acquisition system for fast kinetics. *Nucl. Instrum. Methods* **246**, 452–460 (1986).
5. Baudelet, F. *et al*. ODE: a new beamline for high-pressure XAS and XMCD studies at SOLEIL. *High Pressure Res.* **31**, 136–139 (2011).
6. Strohm, C. *et al*. Multi-frame acquisition scheme for efficient energy-dispersive X-ray magnetic circular dichroism in pulsed high magnetic fields at the Fe K-edge. *J. Synchrotron Rad.* **18**, 224–228 (2011).
7. Newton, M. A., Coldeira, C. B., Inet-Arias, A. M. & Andez-Garcia, M. F. Dynamic in situ observation of rapid size and shape change of supported Pd nanoparticles during CO/NO cycling. *Nat. Mater.* **6**, 528–532 (2007).
8. Abecassis, B., Testard, F., Kong, Q. Y., Francois, B. & Spalla, O. Influence of monomer feeding on a fast gold nanoparticles synthesis: time-resolved XANES and SAXS experiments. *Langmuir*, **26**, 13847–13854 (2010).
9. Hubert, F. *et al*. Growth and overgrowth of concentrated gold nanorods: time resolved SAXS and XANES. *Cryst. Growth & Des.* **12**, 1548–1555 (2012).
10. Rumpf, H., Hormes, J., Moller, A. & Meyer, G. Thermal decomposition of $(NH_4)_2[PtCl_6]$ - an in situ X-ray absorption spectroscopy study. *J. Synchrotron Rad.* **6**, 468–470 (1999).
11. Rumpf, H. *et al*. Thermal decomposition of $(NH_4)_2[PdCl_6]$ studies by in situ X-ray absorption spectroscopy. *J. Synchrotron Rad.* **8**, 707–709 (2001).
12. Verde, Y. *et al*. Pt/C obtained from carbon with different treatments and $(NH_4)_2PtCl_6$ as a Pt precursor. *Applied Catalysis A: General* **277**, 201–207 (2004).
13. Meyer, G. & Moller, A. Thermolysis of ternary ammonium chlorides of rhenium and the noble-metals. *J. Less-Common Met.* **170**, 327–331 (1991).
14. Matuschek, G., Ohrbach, K. H. & Kettrup, A. Simultaneous thermal-analysis mass-spectrometric investigations on the thermal behavior of noble-metal complexes. *Thermochim. Acta*, **190**, 125–130 (1991).
15. Verde-Gomez, Y., Alonso Nunez, G., Cervantes, F. & Keer, A. Aqueous solution reaction to synthesize ammonium hexachloroplatinate and its crystallographic and thermogravimetric characterization. *Mater. Lett.* **57**, 4667–4672 (2003).
16. Weir, R. D. & Westrum, Jr, E. F. Thermodynamics, phase transitions and crystal structure of ammonium hexahalides: comparative study of the heat capacity and thermodynamic properties of $(NH_4)_2PtCl_6$, $(ND_4)_2PtCl_6$, $(NH_4)_2PtBr_6$, $(ND_4)_2PtBr_6$, $(NH_4)_2PdCl_6$, $(ND_4)_2PdCl_6$, $(NH_4)_2TeCl_6$, $(ND_4)_2TeCl_6$, and $(NH_4)_2RuCl_6$ from 5 K to 350 K-a. *J. Chem. Thermodynamics* **34**, 133–153 (2002).
17. Bus, E., Miller, J. T., Kropf, A. J., Prins, R. & van Bokhoven, J. A. Analysis of in situ EXAFS data of supported metal catalysts using the third and fourth cumulant. *Phys. Chem. Chem. Phys.* **8**, 3248–3258 (2006).
18. Clausen, B. S. & Nørskov, J. K. Asymmetric pair distribution functions in catalysts. *Topics in Catalysis* **10**, 221–230 (2000).
19. Lytle, F. W., Sayers, D. E. & Stern, E. A. Extended x-ray-absorption fine-structure technique. II. Experimental practice and selected results. *Phys. Rev. B* **11**, 4825–4835 (1975).
20. Young, D. A. Phase diagrams of the elements. 1975.
21. Fiddy, S. G. *et al*. In situ energy dispersive EXAFS (EDE) of low loaded $Pt(acac)_2/H_I SiO_2$ catalyst precursors on a timescale of seconds and below. *Chem. Commun.* 851–852 (1999).
22. Singh, J., Nachtegaal, M., Alayon, E. M. C., Stötzel, J. & van Bokhoven, J. A. Dynamic structure changes of a heterogeneous catalyst within a reactor: oscillations in CO oxidation over a supported platinum catalyst. *ChemCatChem* **2**, 653–657 (2010).
23. Jentys, A. Estimation of mean size and shape of small metal particles by EXAFS. *Phys. Chem. Chem. Phys.* **1**, 4059–4063 (1999).
24. Ihee, H. *et al*. Ultrafast X-ray diffraction of transient molecular structures in solution. *Science* **309**, 1223–1227 (2005).
25. Chergui, M. Picosecond and femtosecond X-ray absorption spectroscopy of molecular systems. *Acta Cryst.* **A66**, 229–239 (2010).
26. Kong, Q. Y. *et al*. Photolysis of Br_2 in CCl_4 studied by time-resolved X-ray scattering. *Acta Cryst.* **A66**, 252–260 (2010).
27. Kong, Q. Y., Wulff, M., Lee, J. H., Bratos, S. & Ihee, H. Photochemical reaction pathways of carbon tetrabromide in solution probed by picosecond X-ray diffraction. *J. Am. Chem. Soc.* **129**, 13584–13591 (2007).
28. Verde, Y. *et al*. Active area and particle size of Pt particles synthesized from $(NH_4)_2PtCl_6$ on a carbon support. *Catalysis Today* **107–108**, 826–830 (2005).
29. Tolentino, H., Dartyge, E., Fontaine, A. & Tourillon, G. X-ray absorption spectroscopy in the dispersive mode with synchrotron radiation: optical considerations. *J. Appl. Cryst.* **21**, 15–21 (1988).
30. Sutter, J. P., Amboage, M., Hayama, S. & Diaz-Moreno, S. Geometrical and wave-optical effects on the performance of a bent-crystal dispersive X-ray spectrometer. *Nucl. Instrum. Methods A* **621**, 627–636 (2010).
31. Briois, V. *et al*. SAMBA: The 4–40 keV X-ray absorption spectroscopy beamline at SOLEIL. *EDP Sciences* 41–47 (2011).

Acknowledgments

We are very grateful to V. Briois (Beamline SAMBA, Synchrotron Soleil) for the experimental setup of the oven and providing the $PtCl_4$ sample, P. Martinez (group systemes reseaux, Synchrotron Soleil) for the data storage.

Author contributions

Q.K. designed the research; L.B. designed and characterized the oven; Q.K. collected and analyzed data; H.J., O.S. and F.E.P. wrote the Python programs for data analysis; R.G., Q.K., F.B. and S.C. installed and characterized the detector; J.H. wrote the control and data extraction software for the detector; Q.K. and O.S. wrote the manuscript. All authors discussed the results and commented on the manuscript.

Additional information

Supplementary information accompanies this paper at http://www.nature.com/scientificreports

Competing financial interests: The authors declare no competing financial interests.

How to cite this article: Kong, Q. *et al*. Microsecond time-resolved energy-dispersive EXAFS measurement and its application to film the thermolysis of $(NH_4)_2[PtCl_6]$. *Sci. Rep.* **2**, 1018; DOI:10.1038/srep01018 (2012).